iScience, Volume *24*

Supplemental information

Volume-constrained microcontainers enable myoepithelial functional differentiation in highly parallel mammary organoid culture

Michael E. Todhunter, Masaru Miyano, Divya S. Moolamalla, Aleksandr Filippov, Rosalyn W. Sayaman, and Mark A. LaBarge

SUPPLEMENTAL FIGURES

Supplemental Figure 1. Microcontainers enable lrECM-free organoid culture, Related to Figure 1.

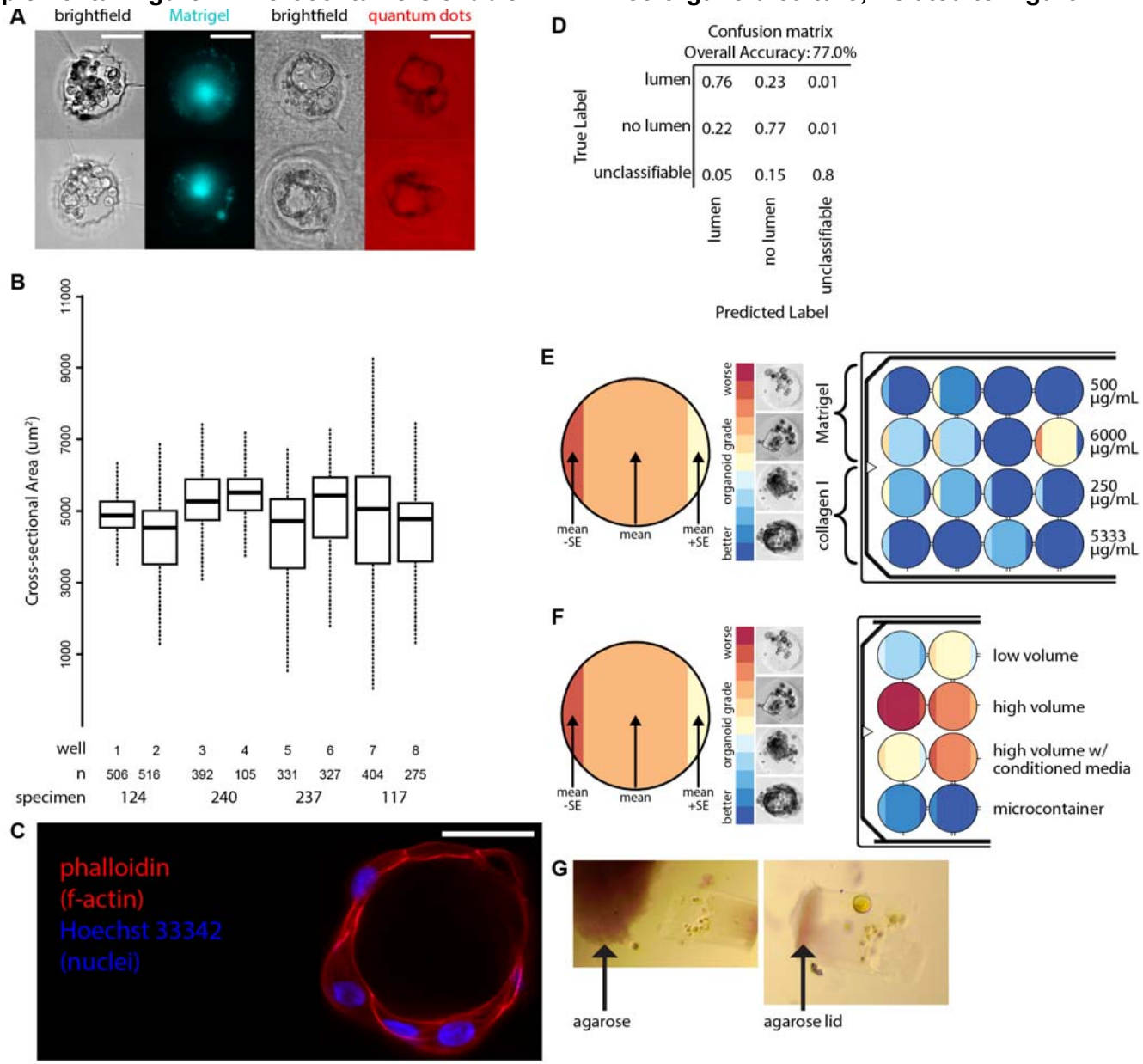

Supplemental Figure 1. (**A**) Microscopy showing the diffusion of different substances from microcontainers after 48h culture. At left, AlexaFluor-594-labeled Matrigel stays within microcontainers. At right, 15 nm diameter quantum dots diffuse freely from the microcontainers. (**B**) Size distribution of organoids in microcontainers, with quadruplicate specimens and technical duplicates, as measured by cross-sectional area. (**C**) A microcontainer organoid with lumen, imaged with confocal microscopy. Scale bar is 50 µm. (**D**) Confusion matrix for random forest binary classifier used to distinguish lumenized from non-lumenized organoids. (**E**) Comparing organoids in supra-gelling and sub-gelling matrices. Organoids were grown in microcontainers loaded with either Matrigel or collagen I at concentrations either below or above the threshold necessary for gelation. After 13 days, morphology was qualitatively assessed, as per the methodology in Fig. 1h-i. (**F**) Comparing organoids in low-volume microwells, high-volume microwells, and high-volume microwells fed with conditioned media from low-volume microwells. After 5 days, morphology was qualitatively assessed, as per the methodology in Fig. 1h-i. (**G**) Staining matrix plugs for agarose content. Lugol's iodine stains agarose purple and leaves protein unstained. After dissecting microcontainers, bulk agarose stains purple, at left. At right, a cylindrical plug of matrix from a microcontainer does not stain purple except for the microcontainer lid.

Supplemental Figure 2. Microcontainer organoids show generally accepted hallmarks of mammary organoids, Related to Figure 2.

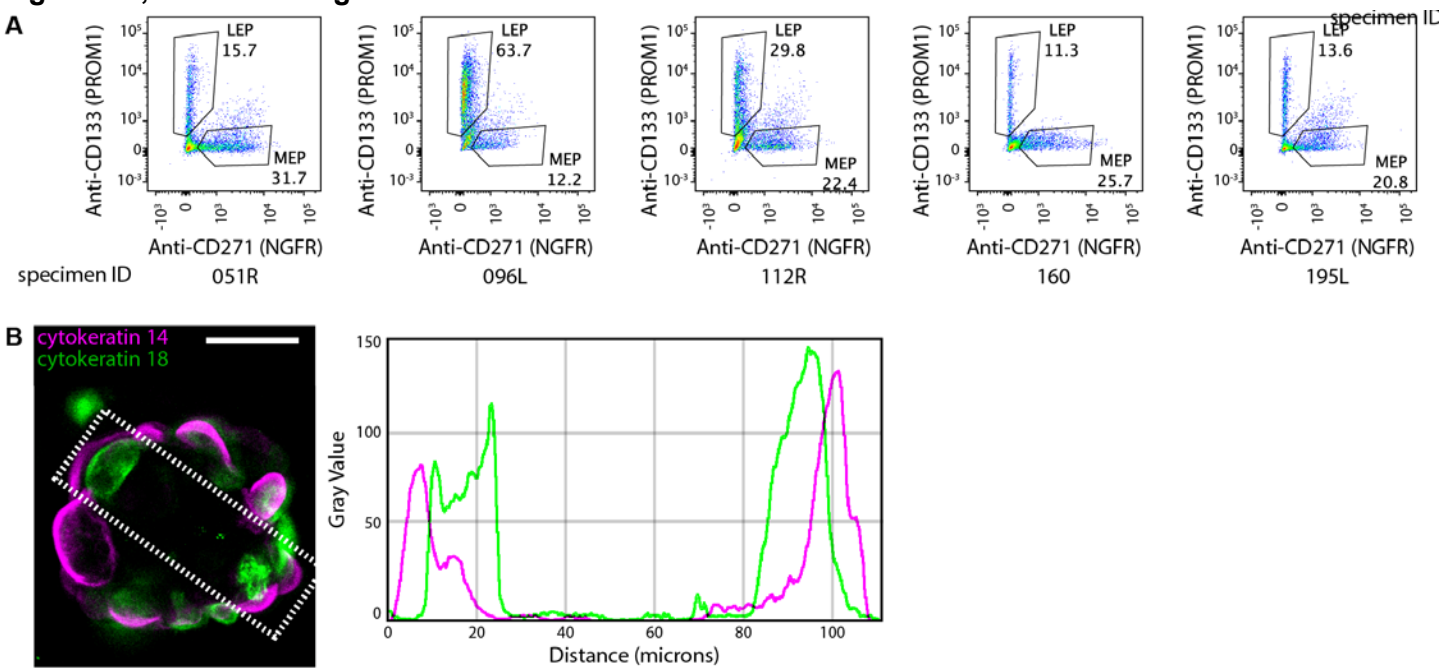

Supplemental Figure 2. (**A**) The lineage composition of various primacy mammary gland specimens, as measured by flow cytometry. CD133 marked luminal cells and CD271 marked myoepithelial cells. (**B**) Line intensity profile showing bilayered stratification of luminal KRT18 and myoepithelial KRT14 from a confocal section of an immunofluorescently stained microcontainer-based HMEC organoid. Scale bar is 50 μm.

Supplemental Figure 3. Mammary organoids grown in microcontainers exhibit contractility, Related to Figure 3.

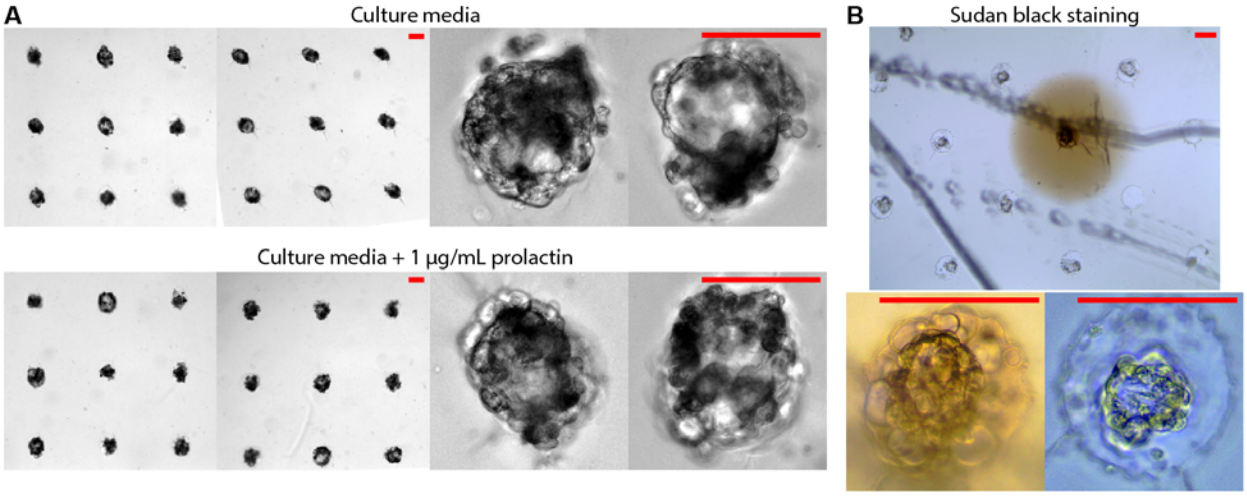

Supplemental Figure 3. (**A**) Morphology of organoids in the presence or absence of prolactin showed no obvious differences with prolactin treatment. (**B**) In one, but only one, case, an organoid and its surroundings stained positive for Sudan Black, a lipophilic dye that stains, among other things, milk secretions. Bottom-left shows a close-up of the sudanophilic organoid, bottom-right shows a non-sudanophilic organoid. Scale bars are 50 µm.

Supplemental Figure 4. Organoids cultured in microcontainers for at least several days retain contractility after transfer to other culture systems,Related to Figure 4.

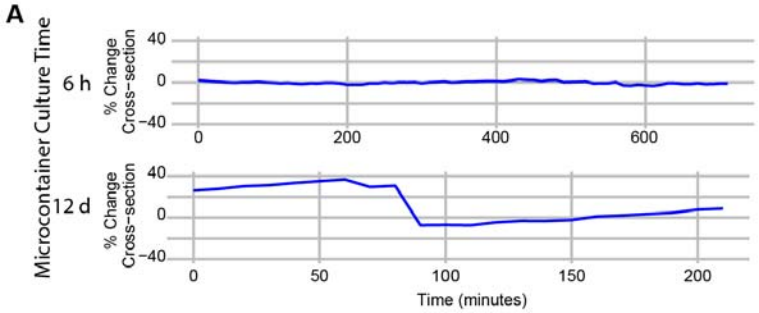

Supplemental Figure 4. (**A**) Alternate time scales for organoids in the Fig. 5B microcontainer transfer experiment. An extended duration (600m) is shown for the 6h organoid, and an abbreviated duration (200m) is shown for the 12d organoid.

Supplemental Figure 5. Gene expression of microcontainer organoids resembles gene expression of primary tissue, Related to Figure 5.

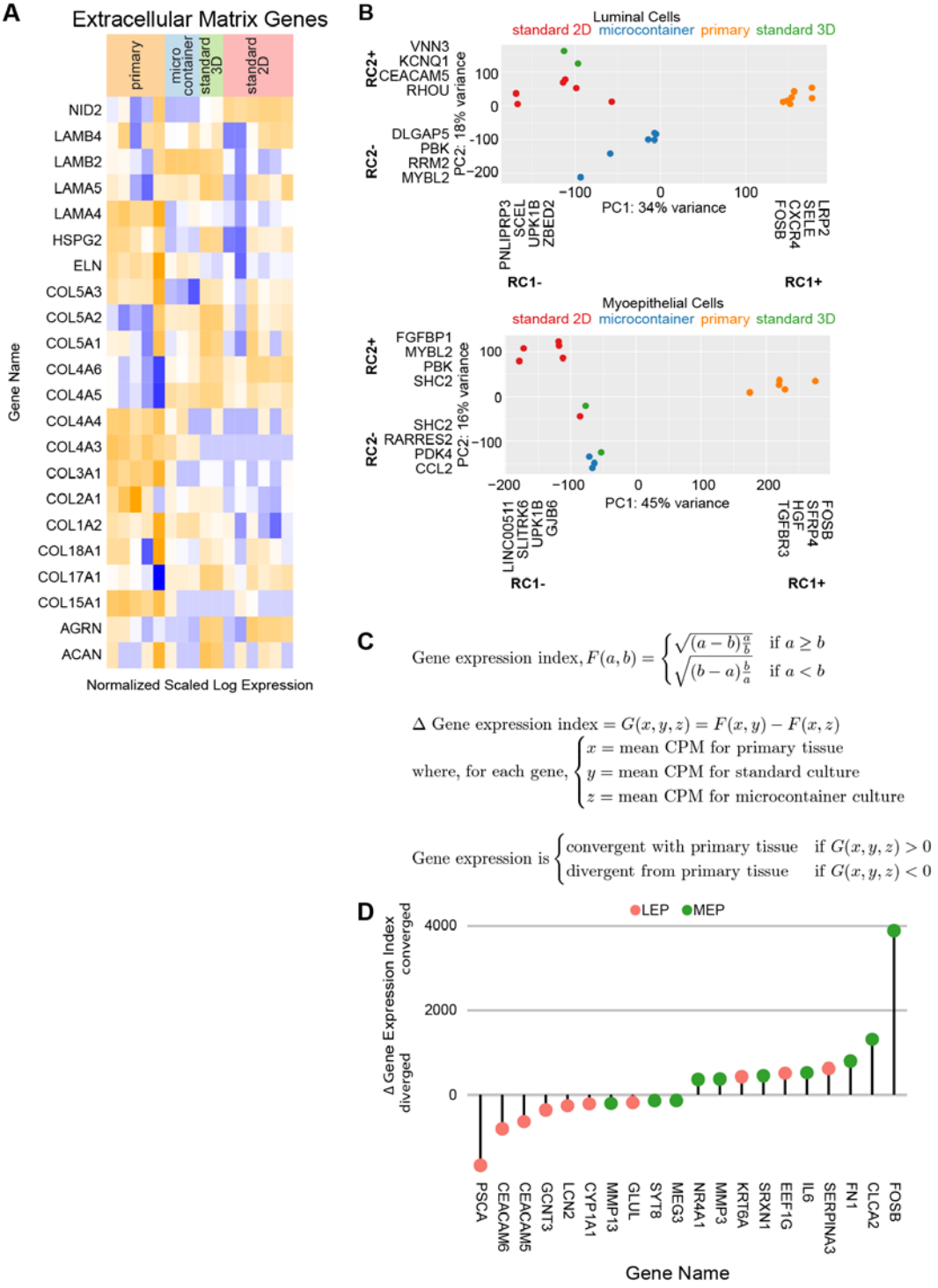

Supplemental Figure 5. (**A**) Relative gene expression for extended list of extracellular matrix genes. (**B**) Principal component analysis of culture conditions, divided by lineage. Genes with the highest loadings for each varimax-rotated component shown along each axis. (**C**) Description of gene expression distance determination. (**D**) Lollipop plot showing the top ten genes whose expression levels most highly converged or diverged from primary tissue, for microcontainers vs standard 3D culture, as per the index described in Fig S3B.

Supplemental Table 1. High-density solutes tested, Related to Figure 1.

Colloids Tested		
within microwell	layered over microwell	
10.0% 4-7 dextrose-equivalent maltodextrin	1.0% IX-A agarose	
15.0% 4-7 dextrose-equivalent maltodextrin	1.0% IX-A agarose	
10.0% 9-13 dextrose-equivalent maltodextrin	1.0% IX-A agarose	poor cell viability
0.0% lipid-rich bovine serum albumin	1.5% IX-A agarose	microwells evacuated of cells
7.5% lipid-rich bovine serum albumin	1.5% IX-A agarose	"donuting" in microwells
10.0% lipid-rich bovine serum albumin	1.0% IX-A agarose	
10.0% lipid-rich bovine serum albumin	2.0% IX-A agarose	"donuting" in microwells
10.0% lipid-rich bovine serum albumin	3.0% IX-A agarose	microwells evacuated of cells
12.5% lipid-rich bovine serum albumin	1.0% IX-A agarose	
15.0% lipid-rich bovine serum albumin	1.0% IX-A agarose	
20.0% lipid-rich bovine serum albumin	1.0% IX-A agarose	challenging to prepare
Colloids Expected to Work		
10.0% bovine serum albumin, fraction V	1.0% IX-A agarose	
10.0% PEG-8000	1.0% IX-A agarose	possible phase separation
10.0% dextran	1.0% IX-A agarose	
10.0% hydroxyethyl starch	1.0% IX-A agarose	

Supplemental Table 2. Matrix compositions tested, Related to Figure 3.

Matrix Compositions						
Matrigel μg/mL	collagen I μg/mL	750 kDa HA μg/mL	2000 kDa HA μg/mL	fibronectin μg/mL	IX-A agarose μg/mL	
0	0	0	0	0	0	
0	250	0	0	0	0	
0	5333	0	0	0	0	gel doesn't flow into microwells
200	0	0	0	0	0	
500	0	0	0	0	0	
750	0	0	0	0	0	
1000	0	0	0	0	0	
1000	500	0	0	0	0	
1000	500	200	0	0	0	
1000	0	200	0	0	0	
1000	0	0	300	0	0	
1000	0	0	1000	0	0	
1000	0	0	3000	0	0	gel doesn't flow into microwells
1000	0	0	0	23	0	
1000	0	0	0	0	100	
1000	0	0	0	0	200	cells don't cohere into organoids
1000	0	0	0	0	400	cells don't cohere into organoids
2000	0	0	0	0	0	
4400	0	0	0	0	0	
6000	0	0	0	0	0	

TRANSPARENT METHODS

General materials and reagents. Reagents were used as received without further purification or modification.

Small molecules. Latrunculin B was purchased from Enzo (cat# BML-T110-0001, lot #8221661). Jasplakinolide was purchased from Enzo (cat# ALX-350-275-C050, lot# 120091480). ML-7 was purchased from Sigma (cat# 12764-5MG, lot# SLBX6943). RepSox was purchased from Sigma (cat# R0158-5MG). SB431542 was purchased from Sigma (cat# 54317-5MG).

Cell culture. Finite-lifespan HMECs were provided by the Human Mammary Epithelial Cell (HMEC) Bank (Stampfer and Garbe, n.d.). For standard 2D culture, primary human mammary epithelial cells at passage 4 were established and maintained in M87A medium as previously described (Garbe et al., 2009). Mycoplasma testing was performed prior to all experiments in this study.

Antibodies and Stains. A comprehensive table of antibodies and stains is below:

Antibodies and Stains

Antibody	Product	Application
anti-human keratin 19	Biolegend 628502 (clone A53-B/A2)	IF (1:1000)
anti-human keratin 14	BioLegend 905301 RB-9020-P (clone Poly9053)	IF (1:1000)
anti-human keratin 18	Novus NBP1-97714	IF (1:1000)
anti-human CD104	Chemicon MAB1964 (clone 3E1)	IF (1:1000)
anti-human laminin, alpha-3	R&D Systems MAB21441 (clone 546215)	IF (1:1000)
anti-human collagen IV	Sigma C1926 (clone COL-94)	IF (1:1000)
anti α-smooth-muscle actin	Sigma A2547 (clone 1A4)	IF (1:1000)
anti-human estrogen receptor	abcam ab16660	IF (1:333)
QTRACKER Qdot vascular labels	Thermo Q21061MP	live (2 μM)
Alexa Fluor 594 NHS ester	Thermo A20004	conjugation
phalloidin iFluor-647	abcam ab176759	FC (1:500)
Hoechst 33342	Thomas Scientific C979U06	FC (1:500)
anti-human CD271, Cy5.5 conjugate	BioLegend 345112 (clone ME20.4)	FC (1:100)
anti-human CD133, PE conjugate	Miltenyl 130-080-801 (clone AC133)	FC (1:50)

Immunofluorescence. Organoids were processed for immunofluorescence while still within microcontainers. All samples were fixed with 4% formaldehyde for 20 min and incubated in blocking buffer (10% heat-inactivated goat serum in PBS+0.5% Triton X-100) at 4 °C for at least 1 day. Primary antibodies were diluted in blocking buffer and added to the sample. After at least 1 day incubating at 4 °C with the primary antibodies,

samples were washed several times with PBS+Triton X-100 for at least 1 day and incubated with fluorophore-conjugated secondary antibodies diluted at a concentration of 1:200 in blocking buffer for approximately 1 day. All samples were washed with PBS+1 μg ml^{-1} DAPI for at least 1 hour before imaging. For widefield imaging, whole organoids were imaged in situ within the microcontainers. For confocal imaging, the agarose lids of the microcontainers were scraped away with a silicone cell scraper, then replaced with a glass coverslip in order to reduce the working distance from the microscope objective.

Flow cytometry. Each sample was transferred to a collection tube and resuspended in PBS. Fluorescently-tagged antibodies were added at concentrations shown in **Table S3** and incubated for 30 minutes on ice. Labeled cells were washed three times with PBS to remove unbound antibody and resuspended in flow buffer (PBS with 2% BSA, 1 mM EDTA, and 1 μg/mL DAPI). Cells were sorted on a BD FacsAria III. LEPs were defined as CD133+/CD10- cells and MEPs were defined as CD133-/CD10+ cells, with DAPI+ cells discarded.

Image acquisition. All confocal microscopy images were acquired using a Zeiss LSM 880 with Airyscan running Zeiss Zen Software. Subsequent deconvolution was performed with AutoQuant. All brightfield microscopy images were acquired using a Nikon Eclipse Ti-E with stage-top incubation and high-speed electro-magnetic stage with piezo Z, running Nikon Elements software. Subsequent workup and image analysis was performed using ImageJ.

Photolithography. Freestanding SU-8 features on silicon wafers were fabricated using standard photolithographic techniques. All recipes used for photopatterning were adapted from MicroChem's technical specification sheets. To obtain cylindrical microwells of 100 μm diameter and 200 μm depth, 60 grams of SU-8 2075 (MicroChem) was spun on a 125 mm technical-grade silicon wafer (UniversityWafer) at 300 rpm for 30 seconds followed by accelerating at 100 rpm/s to a final speed of 700 rpm for 30 seconds. The wafer was soft-baked for 20 minutes at 95 °C, UV-exposed with a 1700 mA 365 nm LED source (ThorLabs) at full power in contact mode for 15 minutes through a photo-mask designed in Adobe Illustrator and purchased from Outputcity Co., post-exposure baked for 5 minutes at 95 °C, and developed in SU-8 developer (MicroChem) for 20 minutes. The patterned substrate was washed with isopropanol/water and baked at 95 °C for 20 minutes. The silicon master was taped to the bottom of a 15 cm Petri dish and potted with Sylgard 184 (Dow Corning). After curing at 65 °C overnight, the molded elastomer was peeled off the wafer and inspected by

microscopy to assess the diameter and depth of the lithographic features. The wafer was rendered hydrophobic by treatment with SigmaCote (Sigma-Aldrich) and subsequent isopropanol washes. At this point, the wafer was ready for production of agarose microwells.

Microcontainer production. Photolithographic masters, prepared as described above, were sanitized with 70% ethanol and kept at 65 °C until use. 20% 5.5 dextrose-equivalent maltodextrin was prepared in 2x PBS and dissolved with gentle heating before 0.2 μm filtration. A solution of 3% agarose in diH_2O was autoclaved and mixed 1:1 with the warm, filtered maltodextrin solution. 15 mL of this mixture was immediately dispensed onto a photolithographic master and allowed to gel at 4 °C. Demolding resulted in agarose microwells. Microwells were equilibrated with cell culture media over two days. Next, HMECs were loaded into microwells by panning and sedimentation. Microwells were inspected by microscopy to confirm cell loading, washed once with cell culture media to remove excess cells, aspirated to near-dryness, and then incubated with 10% 5.5 dextrose-equivalent maltodextrin in cell culture media for 20 minutes at 37 °C. Microwells were again aspirated to near-dryness before being overlaid with 1.0% ultra-low-melting agarose in cell culture media and brought to 4 °C to gelation. Upon gelation of the overlaid agarose, the resulting products are microcontainers. HMEC organoids in microcontainers have their media changed 24 hours after microcontainer formation and once a week thereafter.

Organoid harvesting and RNA isolation. Organoids were harvested from microcontainers prior to RNA isolation. First, the microcontainers were incubated with collagenase for two hours at 37 °C to dissolve any gelled matrix within the microcontainers that would prevent release of the organoids. Next, the microcontainers were inverted with a lab spatula, in order to expose the agarose lids that are otherwise pressed against the tissue culture plastic. Next, the agarose lids of the microcontainers were removed with a silicone cell scraper, exposing the organoids within the opened microcontainers. Next, the tip of a P1000 micropipette was cut to a 1 mm diameter, and PBS was added to a depth of 2 mm over the opened microcontainers. By gently and repeatedly pipetting up and down, the organoids were aspirated out of their microcontainers and transferred to a collection tube.Retrieval of the organoids and corresponding emptying of the microcontainers were verified by microscopy. Approximately 9600 organoids were pooled for each specimen to be analyzed. The retrieved organoids were dispersed into a single-cell suspension with 0.25% trypsin-EDTA and strained through a 40 μm

filter before being LEP and MEP lineages were separated with fluorescence-activated cell sorting, as described above. Total RNA from FACS-sorted cells were isolated using Quick DNA/RNA microprep plus kit (Zymo Research). RNA was submitted to the City of Hope Integrative Genomics Core Facility for library preparation and sequencing.

Image acquisition. All confocal microscopy images were acquired using a scanning confocal microscope (Zeiss LSM 700 running Zeiss Zen software) and deconvolved with AutoQuant. All other microscopy images were acquired using an inverted motorized microscope equipped with live-cell incubation (Nikon Ti-E running Nikon Elements software).

Contraction temporal analysis. Organoid contractions were quantified either by hand or by brightness change analysis, as indicated. For brightness change analysis, time-lapse movies were taken, and the time-derivative of the whole-field image brightness was calculated. Local maxima in the time-derivative were interpreted as contractions and spot-checked by eye. Relevant code is in **Supplemental Code 1.**

Contraction spatial analysis. The Fig. 3 fully contracted diameter measurements were taken by hand. For the Fig. 4 cross-sectional analysis, organoid timelapses were first centered using scale-invariant feature transform (SIFT) and then masked in ImageJ with default settings. Masks were dilated four times, contracted four times, holes filled, and the area of the largest single object was measured over time. Fig. 4B and S4A plot these areas, scaled to the midpoint of their range. Fig. 4C shows, in red, a maximum intensity project of the time-derivative of the whole-field image brightness of these masks, overlaid with a representative image of the organoid in grey.

RNA-seq. RNA library preparation was done with either the KAPA mRNA Hyper kit (cat# KK8581) or the Takara SMART-Seq v4 Ultra Low Input RNA kit (cat# 634888). Sequencing was done on an Illumina HiSeq 2500. Reads were aligned to *Homo sapiens* reference genome hg19 using TopHat2. Unless noted otherwise, exploratory, visualization, and differential gene expression analysis was carried out in R. All relevant code to reproduce the analysis is available in **Supplemental Code 2.** Briefly, for heat maps, raw counts were normalized with the trimmed-means-of-means method then converted to counts-per-million units. For Pearson correlation analysis, any genes with fewer than 100 reads across all specimens were discarded, then DESeq

was used with default settings to identify differentially expressed genes to include in the analysis. Principal component and geometric mean analyses were performed on the entire set of genes. PANTHER inquiries were submitted to http://www.pantherdb.org.

Heart rate variability analysis. Heart rate data was collected with a Polar H7 Bluetooth Heart Rate Sensor using the first author's heart.

Lumenization analysis. Two independent methods were used to assess luemnization. First, organoids were fixed in 4% formaldehyde, stained with phalloidin (for actin) and Hoechst 33342 (for nuclei), and imaged by confocal microscopy. A nucleus-free cavity ringed by phalloidin in the center of an organoid confirmed the presence of a lumen. Second, organoids were classified as lumenized or non-lumenized using a random forest classifier implemented in CellProfiler Analyst. A training set comprising 5% of the image data was manually curated, classifying organoid images as lumenized, non-lumenized, or unclassifiable. Organoid images had a battery of measurements performed on them, which were used as parameters for the random forest classifier. After training, the classifier evaluated all organoids for lumenization at all time points available.

Statistical analysis. For analysis in Fig. 1g-h, 95% confidence intervals (CI) were calculated based on sample standard error (SE) with a finite population correction (FPC). FPC = sqrt(N-n)/(N-1)), where N is the number of organoids in the well (N=300) and n is the number of organoids observed (n=36). Then, SE = sqrt(p*(1-p)/n) * FPC, where p is the fraction of "good" organoids. The margin of error (MOE), where MOE = 1.96 * SE, where 1.96 is the critical value constant for a 95% confidence interval. Finally, the 95% CI was calculated as CI = sample mean +/- MOE.

SUPPLEMENTAL REFERENCES

Garbe, J.C., Bhattacharya, S., Merchant, B., Bassett, E., Swisshelm, K., Feiler, H.S., Wyrobek, A.J., Stampfer, M.R., 2009. Molecular distinctions between stasis and telomere attrition senescence barriers shown by long-term culture of normal human mammary epithelial cells. Cancer Res. 69, 7557–7568.

Stampfer, M.R., Garbe, J.C., n.d. Human Mammary Epithelial Cell (HMEC) Bank [WWW Document]. URL https://hmec.lbl.gov/ (accessed 6.25.20).